

Interplanetary Navigation Using a Continental Baseline for Large Antenna Arrays

Dennis W. Haeberle* and David B. Spencer.†
The Pennsylvania State University, University Park, PA, 16802

Todd A. Ely‡
The Jet Propulsion Laboratory, Pasadena, CA, 91109-8099

Navigation is a key component of interplanetary missions and must continue to be precise with the changing landscape of antenna design. Improvements for the Deep Space Network (DSN) may include the use of antenna arrays to simulate the power of a larger single antenna at much lower operating and construction costs. Therefore, it is necessary to test the performance of arrayed antennas from a navigational point-of-view. This initial investigation focuses on the performance of delta one-way range measurements using a shorter baseline with more data collection than current systems use. With all other parameters equal, the longer the baseline, the better the accuracy for navigation making the number of data packets very important. This trade study compares baseline distances ranging from 1 to 1000 km with an in use baseline, Goldstone to Canberra, of the DSN. The trade study also compares the direction of the baseline, looking at a due east baseline, a due north baseline and a baseline at 45 degrees East of North. The precision of the baseline systems can be found through a simulation created for this purpose using the Jet Propulsion Lab based Monte navigation and mission design tool. The simulation combines the delta one-way range measurements with two-way range and two-way Doppler measurements and puts the measurements through a Kalman filter to determine an orbit solution. Noise is added along with initial errors to give the simulation realism. This study is an important step towards the assessment of the utility of arrays for navigational purposes. The preliminary results have showed a decrease in reliability as the baseline is shortened but the larger continental baselines show comparable results to that of the current Goldstone to Canberra

Nomenclature

a	= Doppler turnaround ratio
B	= DOR baseline
B_x	= DOR baseline vector x-component
B_y	= DOR baseline vector y-component
B_z	= DOR baseline vector z-component
c	= speed of light
f_R	= Doppler frequency shift
f_T	= Transmitter frequency
\vec{l}_i	= ground station state vector
q	= process noise on acceleration
Q	= process noise matrix
r	= magnitude of the vector from the center of the Earth to the spacecraft
$\vec{r}_{s/c}$	= spacecraft position vector
\vec{r}_s	= ground station position vector

* Research Assistant, Department of Aerospace Engineering, 229 Hammond Building, and Student Member.

† Assistant Professor, Department of Aerospace Engineering, 229 Hammond Building, and Associate Member.

‡ Systems Engineer, Navigation and Mission Design, 301-125L, and Senior Member.

\hat{s}	=	unit vector from center of the Earth to the spacecraft
T	=	Doppler step size
w	=	white noise
x_s	=	x-coordinate of the ground station
y_s	=	y-coordinate of the ground station
z_s	=	z-coordinate of the ground station
ρ	=	range
τ_g	=	DOR time measurement

I. Introduction

The Deep Space Network (DSN) is the communications architecture used for interplanetary spacecraft missions. Run by the Jet Propulsion Laboratory (JPL), the network consists of three earth based stations located in Madrid, Spain; Canberra, Australia; and Goldstone, California. At each of these stations there are a number of different antennas consisting of one 34-meter diameter high efficiency antenna and one 34-meter beam waveguide antenna (three at the Goldstone sight), one 26-meter antenna and one 70-meter antenna. These large dishes give the DSN the power to communicate with spacecraft on interplanetary missions throughout the solar system.

The current configuration of the DSN has its share of problems, however. To build new antennas to improve upon those currently available, larger and more expensive antennas would need to be built. The cost of these antennas is driven by their size, with larger antennas requiring larger, more expensive motors and other such components. To alleviate the need for large expensive antennas, studies have begun turning toward antenna arrays using a number of smaller antennas to do the work of a large antenna.

Other benefits of the array structure include an increase in performance, as in the Galileo Mission where scientific data return increased by a factor of three. There is a benefit to the operability in that when deficiencies for a mission arise for a specific size antenna, one could easily partition the array to the size needed. When using single antennas, a deficiency for a 34-meter antenna would require a move to a 70-meter antenna, creating among other things, increased cost and the possibility of over-subscription on the larger antenna. The array format would allow partitioning of the antennas into subsets alleviating the problem of over-subscription. There is also a benefit in the area of flexibility because additional antennas can be added to increase the total aperture as the mission timeline requires. This allows the required cost to be spread over time instead of being levied all at once.¹

As for navigation, there are many questions that need to be answered. In order for the transition to an antenna array to be worthwhile, the tracking accuracy must be at or close to current levels. This accuracy must hold for all mission phases: cruise, launch, orbit insertion, re-entry, and landing. This could be affected by a number of factors including the knowledge of the phase center of the array, using multiple baselines between antennas for measurements instead of the array as a whole or even increased tracking time because the subscription on the antennas is broken up among portions of the array.

There are numerous methods in use to determine the position and velocity of an orbiting spacecraft including, two-way and three-way range, two-way and three-way Doppler, and very long baseline interferometry (VLBI). Two-way and three-way range measurements are simple measurements of distance based on the round trip light time of a signal sent to the spacecraft where in the three-way technique, the signal returns to a second ground station. The two-way and three-way Doppler are techniques that interpret the phase shift of a signal sent to the spacecraft to determine the speed and direction of the spacecraft, where the three-way version again returns to a second ground station. VLBI enlists the services of two stations at very large distances apart on the Earth surface to give a delta one-way range (DOR) measurement normally expressed by time in seconds.² The time represents the difference in time it takes a signal to travel from the spacecraft to the two ground stations a concept that will be explained later.

The focus of this study will be on the use of two-way range, two-way Doppler, and DOR measurements to track the Mars Exploration Rover (MER-B) spacecraft. The key component of the study comes from varying the baseline and varying the data collection variables to determine if a shorter baseline that takes more measurements can be used in place of the intercontinental baseline currently used for DOR measurements. The main idea is to determine if the accuracy of the shorter baseline can be as good as the levels achieved by the long baseline of the current DSN. Given a set of initial conditions the MER-B orbit will be propagated until the orbit determination filter is able to converge. To accomplish the task of simulating the orbit determination process by taking actual measurements a set of partials needs to be developed for each of the three measurement techniques. By using a navigation tool developed at JPL known as the Mission-analysis, Operations, and Navigation Toolkit Environment (MONTE), the orbit determination process will be simulated such that a trade study can be made concerning short baselines for

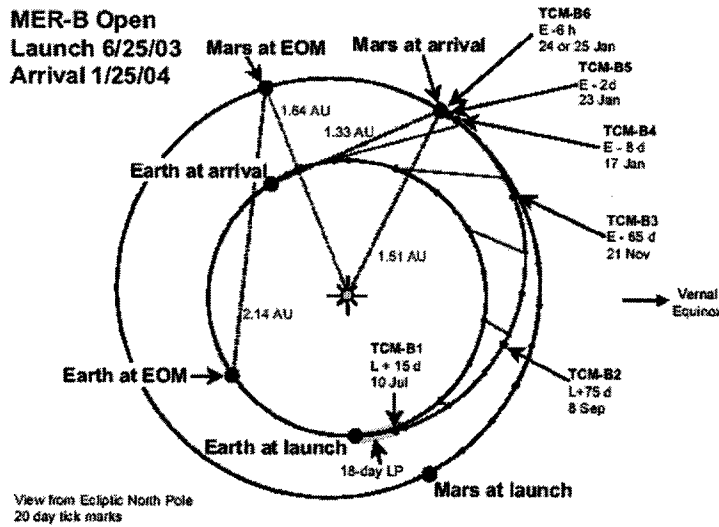


Figure 1. MER-B transfer orbit.³

of Mars to Earth in the summer and fall of 2003. This paper will focus on the approach phase of the Mars transfer orbit beginning approximately 90 days before atmospheric entry and ending approximately 30 days before entry. This time period represents a basic part of the flight and will be used in many more robotic missions to Mars. This maximizes the applicability of this study to future missions for which the DSN will be used.

II. Finding the Partial

To get an accurate representation of observed data, the partial derivatives of each measurement type need to be determined with respect to the state elements of the spacecraft-ground station system. The state vector for this system is made up of twelve elements: the position and velocity terms of the spacecraft in Cartesian coordinates, and the three Cartesian position elements of the ground stations. For two-way Doppler and range, the state elements of the ground station not in use are set equal to zeros.

A. Two-Way Range Partial

The first measurement type is the two-way range. To find the partials, one needs to first look at the Cartesian elements of the range. The range is a vector quantity that represents the difference between the spacecraft position and the ground station position. The range defined in Cartesian coordinates is given by:

$$\vec{\rho} = (x - x_s, y - y_s, z - z_s) \quad (1)$$

The magnitude of the range gives a starting equation for the state partials:

$$\rho = \sqrt{(x - x_s)^2 + (y - y_s)^2 + (z - z_s)^2} \quad (2)$$

Taking the derivative with respect to the first spacecraft state variable, x , results in:

$$\frac{\partial \rho}{\partial x} = \frac{x - x_s}{\sqrt{(x - x_s)^2 + (y - y_s)^2 + (z - z_s)^2}} \quad (3)$$

Similarly the partials for the y and z state variables are:

DOR measurements. Using the shorter baselines, data will be taken more often and at longer intervals. If the measurements with the shorter baselines prove to be as accurate or better than the current DSN setup, it will be the first step in showing that navigation will benefit from the antenna array concept.

MER-B is the second of two rovers sent to Mars to look for signs of water and study the composition of rocks and the surface of Mars. The spacecraft was launched in June of 2003 and arrived at Mars in January of 2004. The flight plan for MER-B is mapped in Fig. 1. Each point represents trajectory correction maneuvers (TCM). The spacecraft followed a short, direct transfer orbit to Mars due to the close proximity

$$\frac{\partial \rho}{\partial y} = \frac{y - y_s}{\sqrt{(x - x_s)^2 + (y - y_s)^2 + (z - z_s)^2}} \quad (4)$$

$$\frac{\partial \rho}{\partial z} = \frac{z - z_s}{\sqrt{(x - x_s)^2 + (y - y_s)^2 + (z - z_s)^2}} \quad (5)$$

From the above equation, one can see that the state partials vector for the position variables is equal to the unit vector of the range, $\hat{\rho}$. The velocity terms do not appear in the equation for the range and therefore, their partials are zero. This allows for a much simpler analysis for range measurements. A similar analysis to that for the spacecraft state variables can be performed to show that the state partials vector for the ground stations is also the unit vector of the range except it is negative. Therefore, finding the range unit vector gives the partials of the state vectors

$$\frac{\partial \vec{\rho}}{\partial r_{s/c}} = \frac{\vec{\rho}}{\rho} = \hat{\rho} \quad (6)$$

$$\frac{\partial \vec{\rho}}{\partial r_s} = -\frac{\vec{\rho}}{\rho} = -\hat{\rho} \quad (7)$$

These partials are multiplied by the state transition matrix of spacecraft states and the Earth rotation matrix of the ground station states, respectively to get the final partials to be used by the simulation.

B. Doppler Partial

Second, the partials for the Doppler measurements need to be derived. This again is fairly simple. The base equation for a Doppler measurement according to the geometrical elements of the observables is:

$$f_R = \frac{2f_T}{cT} \left\{ (1+d)(\rho_k - \rho_{k-1}) + a[(t_x - t_0)(\rho_k - \rho_0) - (t_{x-1} - t_0)(\rho_{k-1} - \rho_0)] \right\} \quad (8)$$

where T is the step size, c is the speed of light, f_T is the transmitter frequency, d and a are constants, and k is any integer greater than zero.

From the previous section and equation 6, it is known that the derivative of the range is its unit vector and because there is a linear relation between f_R and ρ , the range partials are applied here. Thus, the partial vector for the Doppler observable is:

$$\frac{\partial \vec{f}_R}{\partial x} = \frac{2f_T}{cT} (1+d)(\hat{\rho}_k - \hat{\rho}_{k-1}) \quad (9)$$

This can also be applied to the station locations where the partial vector for the range is the negative of its unit vector:

$$\frac{\partial \vec{f}_R}{\partial r_s} = -\frac{2f_T}{cT} (1+d)(\hat{\rho}_k - \hat{\rho}_{k-1}) \quad (10)$$

The state transition matrix and the rotation matrix again come into play here, but this time it is not in the final equation that they are applied. The range partial is multiplied by the state transition matrix before being placed into the equation for the Doppler partials. This also applies to the rotation matrix and the range partials for the ground stations. A noise term, σ_r , is added at the end for more accurate analysis.

C. DOR Partial

The final measurement type need is the DOR measurement. The DOR measurement is the time difference in seconds it takes for a signal sent by a spacecraft to reach two different target ground stations. A visual of a DOR measurement system is represented here to show how the algebraic representation of the time can be inferred through its geometry which can be seen in Fig. 2.

Here B represents the baseline vector between the two ground stations and $\Delta\rho$ is the difference in one way range. Using the geometry above an equation for the delta one way range is derived as²:

$$\Delta\rho = B \cos \theta \quad (11)$$

The right side of the equation can be represented by vectors in the sense that:

$$\Delta\rho = \vec{B} \cdot \hat{s} \quad (12)$$

where \hat{s} is the unit vector in the direction of the spacecraft. In other words, the differenced range is the projection of the baseline in the direction of the spacecraft. In order for this to be true it must be assumed that the ground station-to-spacecraft direction is approximately the same for both stations.

Physically the extra distance traveled can be represented by the time it takes to travel that extra distance multiplied by the speed of the signal:

$$\Delta\rho = \tau_g c \quad (13)$$

This allows for a representation of the measurement in terms of physical parameters that can be differentiated:

$$\tau_g = \frac{1}{c} (\vec{B} \cdot \hat{s}) = \frac{1}{c} \left[\frac{x}{r} B_x + \frac{y}{r} B_y + \frac{z}{r} B_z \right] \quad (14)$$

where $r = \sqrt{(x^2 + y^2 + z^2)}$ and is the distance between the Earth and the spacecraft. Now that there is a representation for the time difference, it now must be differentiated to get the partials starting with the spacecraft state variables. The first partial derived is with respect to x .

$$\frac{\partial \tau_g}{\partial x} = \frac{1}{c} \left[B_x (x^2 + y^2 + z^2)^{-1/2} - x(xB_x + yB_y + zB_z)(x^2 + y^2 + z^2)^{-3/2} \right] \quad (15)$$

Rearranging this equation, the partial becomes:

$$\frac{\partial \tau_g}{\partial x} = \frac{1}{rc} \left[B_x - \frac{x(xB_x + yB_y + zB_z)}{r^2} \right] \quad (16)$$

This same process can be repeated for the y and z partials to get:

$$\frac{\partial \tau_g}{\partial y} = \frac{1}{rc} \left[B_y - \frac{y(xB_x + yB_y + zB_z)}{r^2} \right] \quad (17)$$

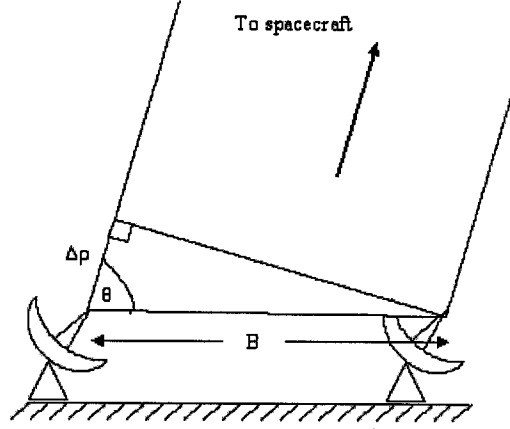


Figure 2. VLBI geometry for observing distant spacecraft.²

$$\frac{\partial \tau_g}{\partial z} = \frac{1}{rc} \left[B_z - \frac{z(xB_x + yB_y + zB_z)}{r^2} \right] \quad (18)$$

Now that the partials for the position have been found, it is necessary to look at the other components of the state vector-the velocity components. Conveniently, there are no velocity components in the DOR measurement equation. This means that all of the velocity partials are zero.

The partials now must be found for the ground stations. First the state vectors need to be defined and linked to the DOR equation. The state vectors are represented by:

$$\begin{aligned} \vec{l}_i &= (l_{ix}, l_{iy}, l_{iz}) \\ i &= 1, 2 \end{aligned} \quad (19)$$

In the DOR equation the station state vectors are represented in the baseline vector term:

$$\vec{B} = \vec{l}_2 - \vec{l}_1 \quad (20)$$

Going back to the DOR equation, the chain rule can be used to generalize the partial. With respect to the x-direction the DOR partial becomes:

$$\frac{\partial \tau_g}{\partial l_{ix}} = \frac{\partial \tau_g}{\partial B_x} \frac{\partial B_x}{\partial l_{ix}} \quad (21)$$

This allows the partial to be taken with respect to the baseline instead of directly with respect to the state variables:

$$\frac{\partial \tau_g}{\partial B_x} = \frac{1}{c} \frac{x}{r} \quad (22)$$

Converting back to the state partials the equation becomes:

$$\frac{\partial \tau_g}{\partial l_{ix}} = \frac{1}{c} \frac{x}{r} \frac{\partial B_x}{\partial l_{ix}} \quad (23)$$

This analysis matches for the other state variables as well. Looking at the baseline equation, the derivative of the baseline is equal to one for station number two and negative one for station number one. So the state vector partials become:

$$\begin{aligned} \frac{\partial \tau_g}{\partial l_{1x}} &= -\frac{1}{c} \frac{x}{r} & \frac{\partial \tau_g}{\partial l_{2x}} &= \frac{1}{c} \frac{x}{r} \\ \frac{\partial \tau_g}{\partial l_{1y}} &= -\frac{1}{c} \frac{y}{r} & \frac{\partial \tau_g}{\partial l_{2y}} &= \frac{1}{c} \frac{y}{r} \\ \frac{\partial \tau_g}{\partial l_{1z}} &= -\frac{1}{c} \frac{z}{r} & \frac{\partial \tau_g}{\partial l_{2z}} &= \frac{1}{c} \frac{z}{r} \end{aligned} \quad (24)$$

These are all the DOR partials needed for the simulator's analysis. For the analysis of the true satellite, a data noise term, σ_d , is added to simulate actual conditions for the signal propagation.

III. Simulation

A. MONTE

MONTE was created at JPL as the next generation software system for spacecraft navigation. MONTE is currently on its third release and will continued to be updated with new simulation tools and new features to accommodate future missions. The intent of MONTE is to provide all trajectory related functions in support of all navigation, from mission planning and design to maintaining and understanding the trajectory data of a current mission.

MONTE contains many built in features to help with navigation studies. One of these features is the orbit propagator. MONTE allows a user to create multiple body systems with initial conditions and then propagate the orbit forward in time. The routine already includes common bodies for spacecraft to orbit including all of the planets in this solar system and many of the moons around these planets. This simulation utilizes the two body system involving the sun and the MER-B spacecraft en route to Mars. More advanced simulations can create systems involving as many objects as deemed necessary by creating more complicated gravity fields and using more accurate perturbations on the orbiting object. MONTE also allows for the placement and propagation of ground station locations on the surface of planets and other bodies. This means that with initial conditions, ground stations can be placed on Earth and will spin with the true spin of the Earth. This is the case with the simulation in this study, with two ground stations on the surface of the Earth at varying locations.

A feature of the orbit propagator is that it stores in a boa file the trajectory information. This allows a user to get information at a specific time during an orbit such as the state variables of the spacecraft or the relative state compared to a ground station or other point in space. This feature is what allows a user to calculate things such as range and range rate or determine if a spacecraft is in view of a ground station. MONTE also allows the user to acquire a state transition matrix for any point in time relative to another point. This is a very important feature because the user can map a state back to an initial condition or map a state forward as a prediction.

B. Simulation Setup

The simulation itself uses many of the built-in features of MONTE. The main features that the simulation utilizes are the orbit propagation tool, the trajectory query tool and the state transition matrix finder. The first step of the simulation uses the orbit propagation tool to create a trajectory library for the spacecraft and the ground stations in use. With the trajectory library created, it is now possible to query any point in the trajectory for information such as relative position, velocity, elevation angles, etc.

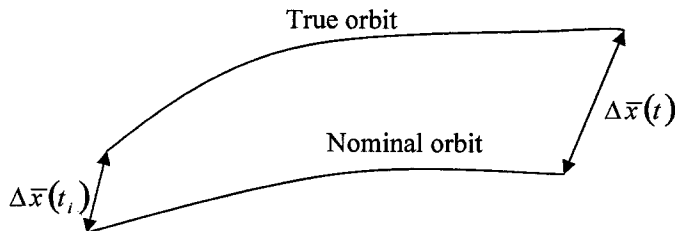


Figure 3. Description of the true and nominal orbits.

Two trajectories are propagated by the simulation. One is the nominal orbit or the actual trajectory of MER-B given the specified initial conditions. The second orbit is that of the true spacecraft. The initial conditions for the nominal orbit are changed by a user defined amount representing the initial knowledge of the spacecraft position. These new initial conditions are propagated

as the true spacecraft position. Both these orbits are illustrated in Fig. 3 with $\Delta\bar{x}$ representing the spacecraft state. The large difference at time t is the reason the filter must take into account initial uncertainties.

Now that the program has a trajectory path to track, the simulation can start its first run. The steps explained here can be followed in Fig. 4. The time loop starts after initializing various filter variables and output lists. On each time step the first task the simulation performs is to check the station schedule to determine if any measurements should be taken. If it has been long enough since the last measurements, the program checks to see if the stations are in view of the spacecraft. If both are in view and the schedule calls for a DOR measurement, the DOR measurement is taken. If one station is in view and the schedule calls for a Doppler or range measurement, these measurements are taken. The program then uses subroutines to obtain the actual measurements of the true and nominal spacecraft trajectories as well as the partial derivatives of the DOR measurement with respect to the state vectors. These values are then fed into an initial state Kalman filter which maps the current conditions back to an original state which is updated every time the filter is called. The filter outputs an error and a covariance associated with the position error of the spacecraft. At the end of the two month track, these values are plotted and saved.

The user has many options when running this program. There are a large number of inputs defined in the initialization file and the data collection routine. The user must define the initial conditions of the spacecraft orbit using Cartesian position and velocity components as well as the reference frame and center body of the orbit. Also the station locations need to be specified by their geodesic coordinates: latitude, longitude and altitude. In relation to these initial conditions, the user must specify an uncertainty associated with the initial conditions to create the true spacecraft state. In order for the propagator to create the spacecraft's trajectory, the program needs the initial epoch and the duration time of the simulation.

The tracking scheduler needs information about the time intervals between measurement passes, the time interval between individual measurements and the length of tracking pass. Each individual tracking technique has its own set

of these parameters. The tracking techniques, Doppler, range and DOR, can be toggled on and off in the initiation file giving the user a way to study the effects of individual measurement types on solution accuracy. Each measurement type has a data weight associated with it, again something that can be changed to suit a specific simulation.

Errors on the state variables of the spacecraft and the stations have an effect on the way the filter performs and converges. The program is set up to allow the user to toggle the state variables on and off such that they do not contribute to any errors in state system. This can be useful in determining the sensitivity of the filter to specific state variables and allowing states that are of no interest to be toggled off. Each state is then given an error to simulate process noise. This is done for the spacecraft by feeding the program an acceleration error which is then used to calculate process noise on the position and velocity states at each time step. In order to find the process

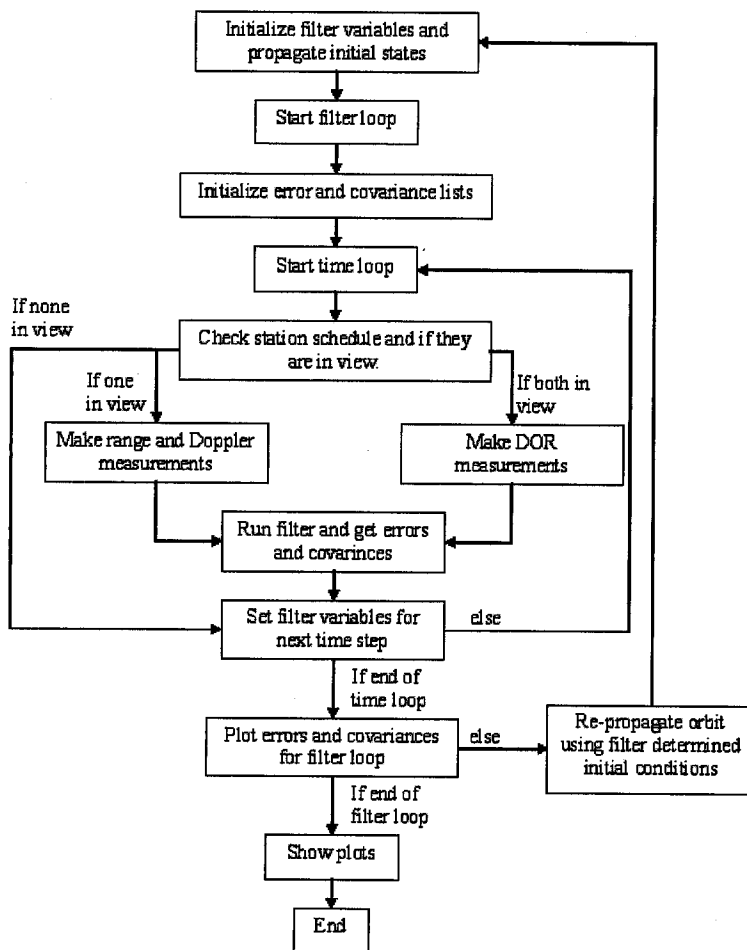


Figure 4. Flow chart for spacecraft navigation simulation.

noise on the position and velocity, the state equation must be looked at first.

$$\begin{bmatrix} \dot{\vec{x}} \\ \dot{\vec{v}} \end{bmatrix} = [A] \begin{bmatrix} \vec{x} \\ \vec{v} \end{bmatrix} + \begin{bmatrix} 0 \\ w \end{bmatrix} \quad (3.1)$$

$$[A] = \begin{bmatrix} 0 & 1 \\ 0 & 0 \end{bmatrix}$$

where w is the white noise. Using the state relation:

$$\dot{P} = AP + PA^T + Q \quad (3.2)$$

and substituting, we get:

$$\begin{bmatrix} \dot{p}_{11} & \dot{p}_{12} \\ \dot{p}_{21} & \dot{p}_{22} \end{bmatrix} = \begin{bmatrix} 0 & 1 \\ 0 & 0 \end{bmatrix} \begin{bmatrix} p_{11} & p_{12} \\ p_{21} & p_{22} \end{bmatrix} + \begin{bmatrix} p_{11} & p_{12} \\ p_{21} & p_{22} \end{bmatrix} \begin{bmatrix} 0 & 0 \\ 1 & 0 \end{bmatrix} + \begin{bmatrix} 0 & 0 \\ 0 & q \end{bmatrix} \quad (3.3)$$

where q is the user specified process noise on the acceleration and the p values need to be determined. By multiplying the matrices the equation becomes:

$$\begin{bmatrix} \dot{p}_{11} & \dot{p}_{12} \\ \dot{p}_{21} & \dot{p}_{22} \end{bmatrix} = \begin{bmatrix} p_{11} & p_{12} \\ 0 & 0 \end{bmatrix} + \begin{bmatrix} p_{11} & 0 \\ p_{21} & 0 \end{bmatrix} + \begin{bmatrix} 0 & 0 \\ 0 & q \end{bmatrix} \quad (3.4)$$

This leads to a set of four differential equations:

$$\begin{aligned} \dot{p}_{11} &= p_{21} + p_{12} & \dot{p}_{12} &= p_{22} \\ \dot{p}_{21} &= p_{22} & \dot{p}_{22} &= q \end{aligned} \quad (3.5)$$

Beginning with $\dot{p}_{22} = q$, the differential equations can easily be solved to arrive at a solution for the white noise:

$$Q(t) = \begin{bmatrix} p_{11} & p_{12} \\ p_{21} & p_{22} \end{bmatrix} = \begin{bmatrix} \frac{1}{3}qt^3 & \frac{1}{2}qt^2 \\ \frac{1}{2}qt^2 & qt \end{bmatrix} \quad (3.6)$$

Or in a 6x6 matrix for the actual spacecraft state variables:

$$Q(\Delta t) = \begin{bmatrix} \frac{1}{3}q_x\Delta t^3 & 0 & 0 & \frac{1}{2}q_x\Delta t^2 & 0 & 0 \\ 0 & \frac{1}{3}q_y\Delta t^3 & 0 & 0 & \frac{1}{2}q_y\Delta t^2 & 0 \\ 0 & 0 & \frac{1}{3}q_z\Delta t^3 & 0 & 0 & \frac{1}{2}q_z\Delta t^2 \\ \frac{1}{2}q_x\Delta t^2 & 0 & 0 & q_x\Delta t & 0 & 0 \\ 0 & \frac{1}{2}q_y\Delta t^2 & 0 & 0 & q_y\Delta t & 0 \\ 0 & 0 & \frac{1}{2}q_z\Delta t^2 & 0 & 0 & q_z\Delta t \end{bmatrix} \quad (3.7)$$

where:

$$\Delta t = t - t_{lm} \quad (3.8)$$

where t_{lm} is the time of the last measurement taken. The process noise on the station locations is assigned as a constant at the beginning of the simulation and is not affected by time. For this particular orbit, the process noise on the acceleration is set to $(3 \times 10^{-9})^2$ and the process noise on the stations is set at $(1 \times 10^{-6})^2$.

C. Trade Study

For a comparison to the current system, there needs to be a standard case for comparison. The base case for this study will be an in-place measurement system using two-way range, two-way Doppler, and DOR along a baseline

between Goldstone and Canberra. The parameters for this base case include a number of things in the way of data collection. The two-way Range measurements will be taken twice a day for four hours, one at each DSN station. The tracks will have a data interval of 30 minutes and a data weight of 1 meter. Also the simulation will have a range bias of a 100 meter a priori uncertainty. The two-way Doppler measurements will also be taken twice a day for four hours, once at each DSN station. These measurements will have a data interval of 10 minutes and a data weight of 0.075 mm/s. The DOR measurements will be taken twice a week. Each track will be performed at the same DSN stations with a data weight of 5 nanoseconds. The baseline case will be run until filter convergence with an initial conditions error on the order of 10 km, and station location errors on the order of 1 cm. Once the basic case is performed, the study will move into the investigation of shorter baselines.

The second part of the study will involve two ground stations, Goldstone and a station whose location varies by distance and direction relative to Goldstone. A number of distance cases will be looked at in three directions: due East, due North, and forty-five degrees Northeast. In each direction, the study looks at baselines of 2000 km, 1000 km, 500 km, 100 km, 10 km, and 1 km. The lowest of these distances will enhance the possibility of putting an array at a single facility. Longer baselines normally provide the best results for VLBI, so in these cases there needs to be another measurement variable changed to improve or maintain current accuracy. This variable is the frequency of measurements taken by the DSN stations. The shorter baseline cases will take measurements in two cases: once a day and twice a day. That gives the shorter baseline cases up to 7 times more data points than the intercontinental baseline. There will also be three data weights investigated for each geometry: 5 nanoseconds, 1 nanosecond and 0.1 nanoseconds. The other two measurement methods, two-way range and two-way Doppler, will maintain the same parameters for taking measurements. This is to be expected because they only utilize one station at a time in all of the cases including the base case. Also, using the North-East baseline direction cases, a one-to-one comparison will be made with the basic case (same measurement parameters).

IV. Preliminary Results

The presented results are based on the previously described trade study with some noted changes. First, only one data weight for DOR was looked at for the continental baseline as well as only one data sampling rate for DOR. Also, the DOR only cases will be done later. Finally the preliminary results give an overall accuracy of each tracking simulation while the final trade study will be broken into B-plane components. For the baseline case there were two cases run: one with Doppler and range only and the other with Doppler, range and DOR measurement types. As will be the standard for all cases, the results are plots of the error versus time. There are two curves on these plots, one being the observed error and the other the covariance.

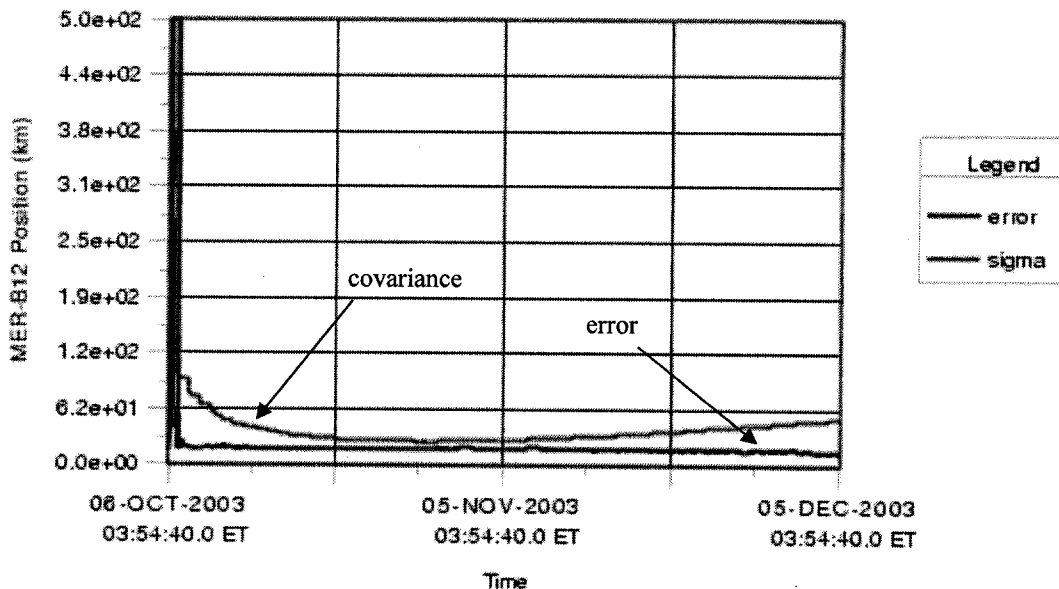


Figure 5. Accuracies for a Goldstone-Canberra baseline using all measurement types.

The baseline case, in Fig. 5 shows the accuracy of the current system using two DOR measurements per week. The simulation covariance converged to roughly 30 km. The observed error by the intercontinental baseline converged to approximately 20 km. These results are in a very good range and once converted to the B-plane should compare favorably to the reported accuracy of the MER-B mission. The Doppler and range only case for the intercontinental baseline, Fig. 6, loses accuracy when compared to the use of DOR measurements. As seen the covariance converges to approximately 56 km while the error converges near 30 km. The loss in accuracy is to be expected due to the added measurement type. The difference was expected to be more, but the case with DOR measurements did appear to converge faster as well as to its more accurate result.

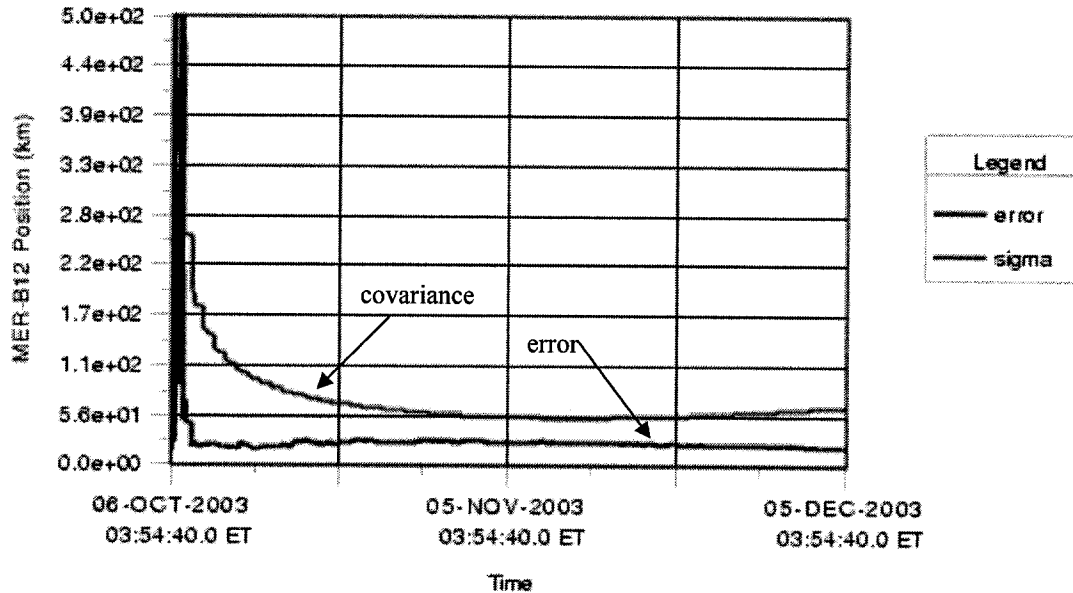


Figure 6. Accuracies for a Goldstone-Canberra baseline using Doppler and Range only.

Figures 7-9 show the results of a 1000 km continental baseline for the three directions of the trade study. As can be seen by these figures, the results are not as accurate as those from the baseline case but are still within a reasonable range. Of particular note is the fact that the north and northeast baselines are approximately twice as accurate as the east baseline. In fact the north and northeast baseline compare very favorably to the baseline case. This shows that for a particular orbit, the baseline direction can have a significant effect on the accuracy of the orbit determination.

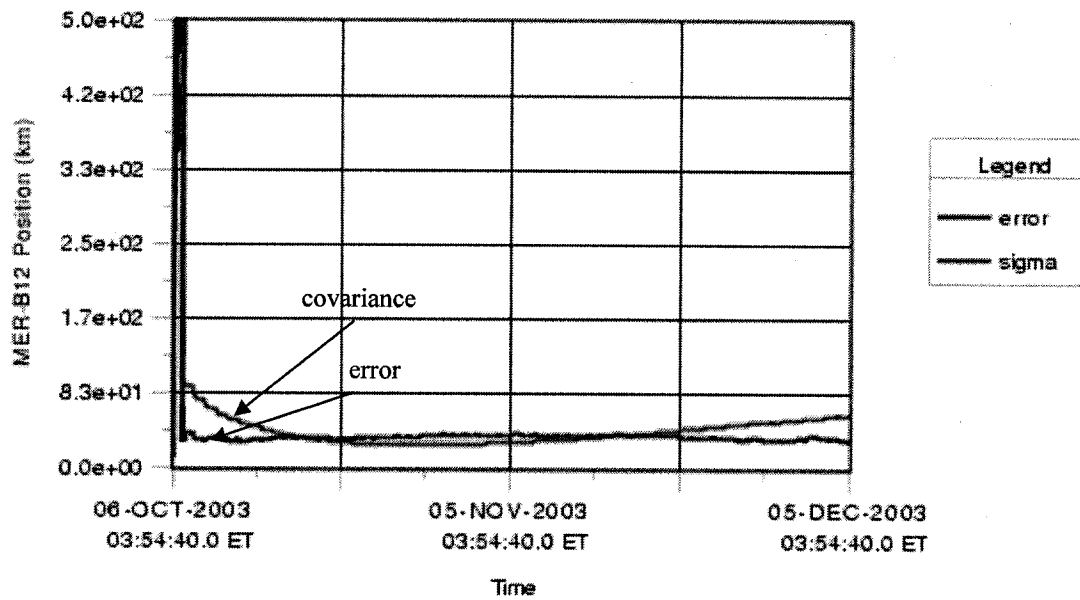


Figure 7. Accuracies for a 1000 km-North baseline.

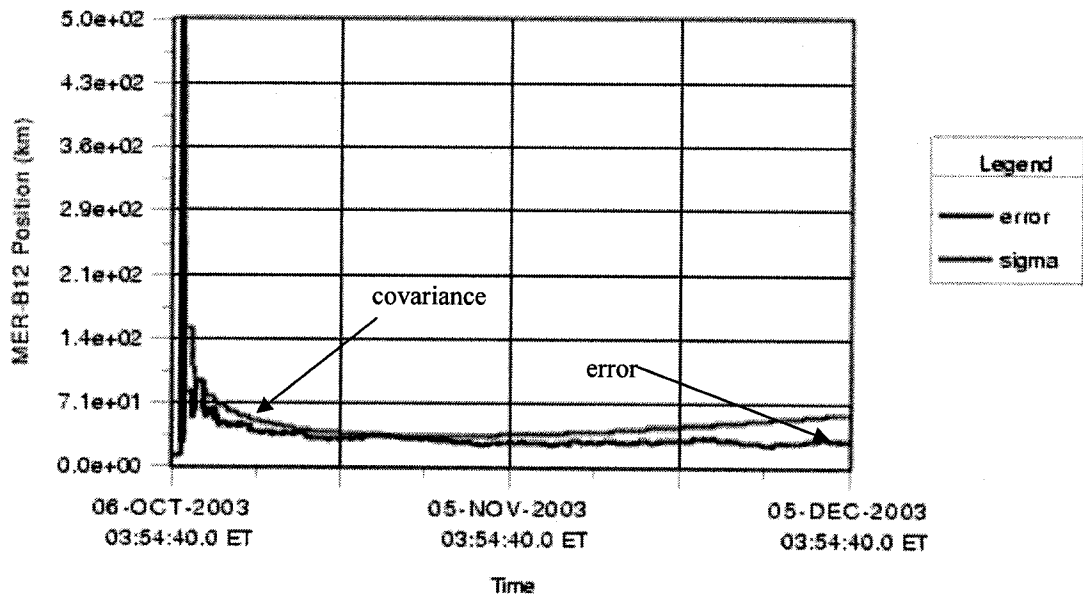


Figure 8. Accuracies for a 1000km-Northeast baseline.

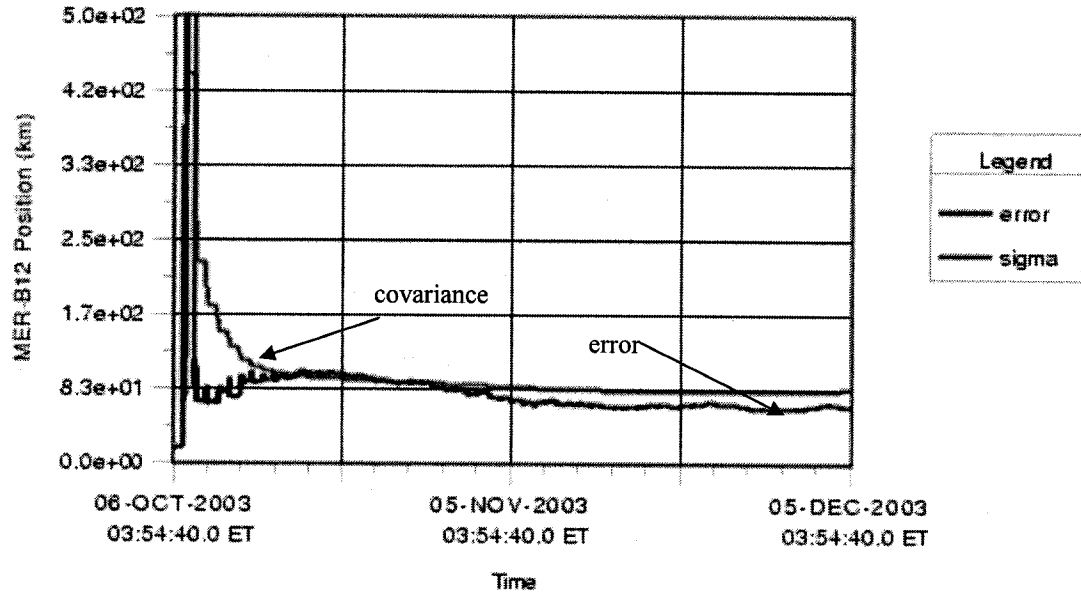


Figure 9. Accuracies for a 1000 km-East baseline.

Figures X10 and X11 show the results of a 1 km and 500 km baseline to the east. These, along with the results of the 1000 km baseline in Fig. 9, show how the navigational accuracy changes as a function of the baseline length. These three plots show a distinct downward trend in accuracy as the baseline gets smaller. This relation is to be expected due to the fact that large baselines provide a more consistent DOR time giving the observer a better resolution of the pointing vector. The numbers range from an error of a covariance of around 83 km and an observed error of approximately 60 km in the 1000 km baseline case to the a covariance and error near 100 km and 75 km, respectively. The drop-off was expected to be larger making this small range very interesting. An interesting note is that the 1 km baseline case, a case that puts both ground stations within a single complex, were all close to, if not exactly the same, result. This can be interpreted to mean that the smaller baselines depend very little on the direction of the baseline but may also mean that the DOR measurements have very little effect on the accuracy.

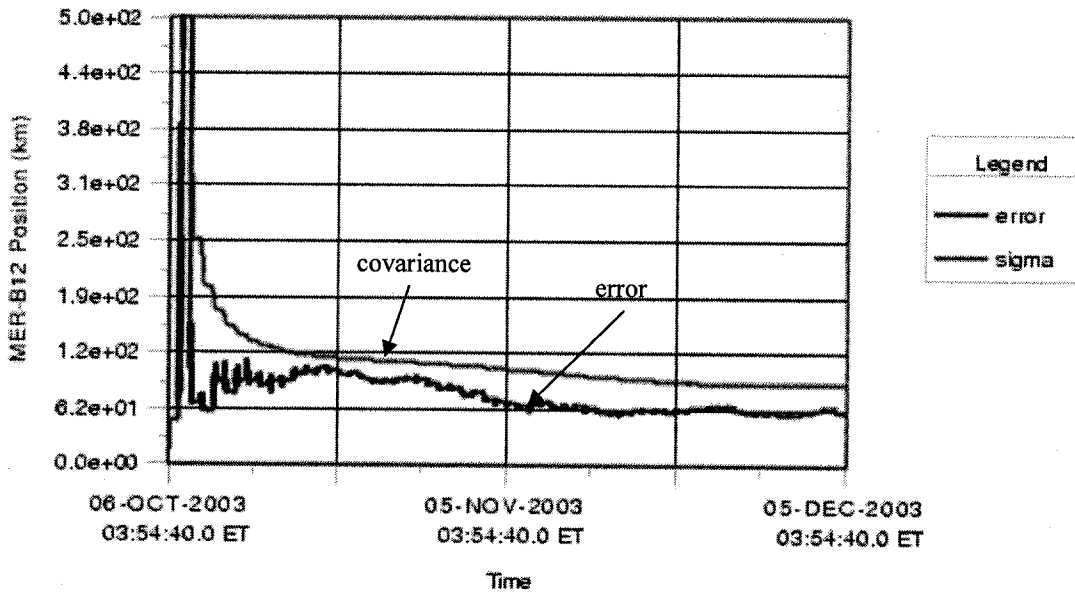


Figure 10. Accuracies for a 500 km-East baseline.

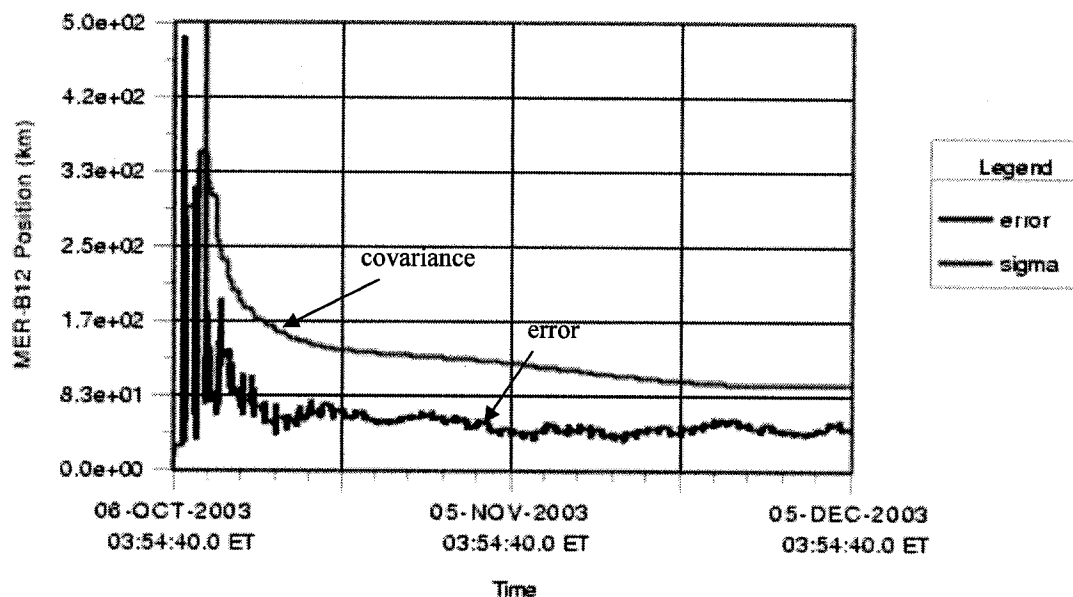


Figure 11. Accuracies for a 1 km-East baseline.

V. Conclusions and Future Work

The preliminary results of this study show many of the tendencies of navigational accuracies in regards to baseline variables. These results are valuable but a completed trade study will provide much more information than can be found in these preliminary findings. The baseline cases tell us just how much affect the DOR measurements are having on the accuracy of the filter. They prove that DOR measurements are important pieces of data in resolving the orbit of a spacecraft. The continental baseline cases showed that decreasing the baseline most assuredly decreases the accuracy of one's measurements. This can be seen through the comparison of the east baselines in Fig. 9-11. The continental baseline results also showed that for larger baselines, the accuracy of the filter is also dependent on the baseline direction.

The future of this study lies in the completion of the trade study described in the simulation section of this paper. The program needs to be modified to output results in B-plane coordinates so that a more thorough conclusion can be reached. Once the trade study has been completed, the benefits of very short baselines can be assessed in their application to antenna arrays. The simulation can be extended to include multiple baselines for better results. The study will also be extended to look at other mission phases including take-off, orbit insertion and landing of interplanetary spacecraft, to go along with this current study of the cruise/approach phase. Extending this simulation will give insight into the navigational benefits of a large antenna array located in a single complex and will help determine if the large arrays are viable beyond scientific data collection.

Acknowledgments

The authors would like to thank the NASA Jet Propulsion Laboratory for providing many resources including the MONTE program, computing time and very knowledgeable colleagues.

References

- ¹Thornton, Catherine L., Border, James S, "Radiometric Tracking Techniques for Deep-Space Navigation," Deep Space Communications and Navigation Series, JPL Publication 00-11, Oct. 2000.
- ²D. H. Rogstad, A. Mileant, T. T. Pham. *Antenna Arraying Techniques in the Deep Space Network*. Monograph 5, Deep Space Communications and Navigation Series. JPL Publications 03-001, Jet Propulsion Laboratory, Pasadena, California, January, 2003
- ³"Mars Exploration Rover Mission Plan," MER 420-1-301, JPL D-19660, February 20, 2002